

Chiral three-nucleon interaction and the ^{14}C -dating β decay

J. W. Holt, N. Kaiser, and W. Weise

Physik Department, Technische Universität München, D-85747 Garching, Germany

(Received 2 February 2009; revised manuscript received 9 April 2009; published 29 May 2009)

We present a shell-model calculation for the β decay of ^{14}C to the ^{14}N ground state, treating the relevant nuclear states as two $0p$ holes in an ^{16}O core. Employing the universal low-momentum nucleon-nucleon potential $V_{\text{low } k}$ only, one finds that the Gamow-Teller matrix element is too large to describe the known (very long) lifetime of ^{14}C . As a novel approach to this problem, we invoke the chiral three-nucleon force (3NF) at leading order and derive from it a density-dependent in-medium NN interaction. By including this effective in-medium NN interaction, the Gamow-Teller matrix element vanishes for a nuclear density close to that of saturated nuclear matter, $\rho_0 = 0.16 \text{ fm}^{-3}$. The genuine short-range part of the three-nucleon interaction plays a particularly important role in this context, since the medium modifications to the pion propagator and pion-nucleon vertex (owing to the long-range 3NF) tend to cancel out in the relevant observable. We discuss also uncertainties related to the off-shell extrapolation of the in-medium NN interaction. Using the off-shell behavior of $V_{\text{low } k}$ as a guide, we find that these uncertainties are rather small.

DOI: [10.1103/PhysRevC.79.054331](https://doi.org/10.1103/PhysRevC.79.054331)

PACS number(s): 21.45.Ff, 21.30.Fe, 23.40.-s, 27.20.+n

I. INTRODUCTION

The anomalously long β decay lifetime of ^{14}C , which makes possible the radiocarbon dating method, has long been a challenge to nuclear structure theory. The transition from the $J_i^\pi = 0^+$, $T_i = 1$ ground state of ^{14}C to the $J_f^\pi = 1^+$, $T_f = 0$ ground state of ^{14}N is of the allowed Gamow-Teller type, yet the known lifetime of $\sim 5730 \pm 30$ years is nearly six orders of magnitude longer than would be expected from typical allowed transitions in p -shell nuclei [1,2]. The associated Gamow-Teller (GT) transition matrix element for the ^{14}C decay must therefore be accidentally small, on the order of 2×10^{-3} , which makes this transition a sensitive test for both nuclear interaction models and nuclear many-body methods.

The earliest studies to give insight into this problem were based on phenomenological models of the residual nuclear interaction. If only central and spin-orbit forces are included, it can be shown [3] that it is impossible to achieve a vanishing GT matrix element when the model space is restricted to $0p^{-2}$ configurations consisting of two $0p$ holes in an ^{16}O core. Later, Jancovici and Talmi [4] discovered that this problem can be overcome with the addition of a tensor force component in the residual interaction. When realistic nuclear forces based on meson exchange were developed in the 1960s and applied to nuclear many-body problems through the G -matrix formalism, Zamick [5] found the decay rate to be very sensitive to the $0p_{1/2}$ - $0p_{3/2}$ splitting, with overall unsatisfactory results when the experimental value of 6.3 MeV is used. A more recent calculation [6] of the ^{14}C β decay has been performed in a large-basis no-core shell-model study performed with the Argonne V8' interaction [7]. Although it was shown that the inclusion of additional configurations up to $6\hbar\omega$ lead to a suppression of the GT matrix element, the results were not yet converged at this order.

Very recently, it has been suggested [8] that the ^{14}C β decay transition matrix element should be particularly sensitive to the density dependence of the nuclear interaction. The study in Ref. [8] used a medium-dependent one-boson-exchange

nuclear interaction modeled with Brown-Rho scaling [9,10], in which the masses of the bosons (except the pion) decrease in a nuclear medium owing to either normal hadronic many-body effects or the partial restoration of chiral symmetry at finite density. In the present work, we examine the role of density-dependent corrections to the nuclear interaction from the leading-order chiral three-nucleon force (3NF) at one-loop order. For the density-independent two-body part of the interaction we use the low-momentum interaction $V_{\text{low } k}$ derived from the Idaho next-to-next-to-next-to-leading-order (N^3LO) chiral potential [11,12] for cutoffs between $\Lambda_{\text{low } k} = 2.1$ and 2.3 fm^{-1} . For densities in the neighborhood of saturated nuclear matter ($\rho_0 = 0.16 \text{ fm}^{-3}$), we find a large suppression of the GT matrix element that is almost entirely due to the short-range component of the chiral 3NF. There are three contributions arising from the long-range two-pion exchange component of the chiral 3NF, but the largest two terms approximately cancel. Moreover, we find that the density-dependent corrections resulting from the medium-range 3NF are naturally small. We also calculate the Gamow-Teller strengths from the ground state of ^{14}N to the excited states of ^{14}C and find that they are in satisfactory agreement with recent experimental data [13], although generally they are much less sensitive to the density dependence of the nuclear interaction than the ground state to ground state transition.

The present paper is organized as follows. In Sec. II we develop a model for the density-dependent nucleon-nucleon (NN) interaction in medium. For the density-independent part, we use model space/renormalization group techniques to construct a low-momentum two-body nuclear interaction based on the N^3LO chiral NN potential. We then present analytic expressions for the six unique density-dependent contributions to the in-medium NN interaction derived from the leading-order chiral 3NF at one-loop order. As suggested in Ref. [14], the two low-energy constants, c_D and c_E , of the medium- and short-range chiral 3NF are chosen to reproduce the binding energies of light nuclei for a given low-momentum scale $\Lambda_{\text{low } k}$.

In Sec. III we present the results of our shell-model calculation, and in Sec. IV we give a brief summary and outlook.

II. IN-MEDIUM NUCLEAR INTERACTION

A. Free-space low-momentum nucleon-nucleon interaction

For many years there has been much effort devoted to the construction of realistic models of the nuclear interaction; these are important not only for understanding the properties of normal nuclei but also for constraining the structure of dense stellar objects such as neutron stars. The underlying assumption of these models is that the nuclear force arises primarily from the exchange of various mesons, though the choice of which mesons to include and how to account for the strong short-distance repulsion in the NN interaction are largely model dependent. Nevertheless, various models containing between 30 to 40 free parameters (typically meson masses, coupling constants, and form factor cutoffs) are able to reproduce all of the experimental pp and pn scattering phase shifts below a laboratory energy of 350 MeV, as well as the properties of the deuteron, with a χ^2 per degree of freedom of about 1.

Recently, a program has been developed [15,16] to understand the scale dependence of the NN interaction from the point of view of effective field theory and the renormalization group. Since the short-distance behavior of the NN interaction is not constrained experimentally, renormalization group techniques have been used in Refs. [15,16] to evolve these (bare) NN interactions down to the scale at which our experimental information stops, that is, around a center-of-mass momentum $p \simeq \Lambda_{\text{low } k} \simeq 2.1 \text{ fm}^{-1}$. These low-momentum interactions, $V_{\text{low } k}$, are phase-shift equivalent to the underlying bare interaction up to a predefined cutoff scale $\Lambda_{\text{low } k}$. As the decimation scale is reduced to $\Lambda_{\text{low } k} \simeq 2.1 \text{ fm}^{-1} \simeq 400 \text{ MeV}$, all of these low-momentum interactions flow to a nearly universal interaction. The method for constructing such an interaction is explained in the following.

One begins with the half-on-shell T -matrix¹ for free space scattering,

$$T(p', p) = V_{NN}(p', p) + \frac{2}{\pi} \mathcal{P} \int_0^\infty \frac{V_{NN}(p', q)T(q, p)}{p^2 - q^2} q^2 dq, \quad (1)$$

from which one defines a low-momentum half-on-shell T -matrix by

$$T_{\text{low } k}(p', p) = V_{\text{low } k}(p', p) + \frac{2}{\pi} \mathcal{P} \int_0^{\Lambda_{\text{low } k}} \frac{V_{\text{low } k}(p', q)T_{\text{low } k}(q, p)}{p^2 - q^2} q^2 dq, \quad (2)$$

where \mathcal{P} denotes the principal value and the cutoff $\Lambda_{\text{low } k}$ is *a priori* arbitrary. To preserve phase shifts, where $\tan \delta(p) = -pT(p, p)$, one requires that these two T -matrices be equal

for relative momenta less than the cutoff $\Lambda_{\text{low } k}$,

$$T_{\text{low } k}(p', p) = T(p', p), \quad \text{for } p', p < \Lambda_{\text{low } k}, \quad (3)$$

a condition that defines the low-momentum potential $V_{\text{low } k}$. It can be shown [15] that a solution to these equations is given by the Kuo-Lee-Ratcliff folded diagram effective interaction [17,18]. There are several schemes [19,20] available for accurately computing $V_{\text{low } k}$, and each scheme preserves the deuteron properties. Under this (scale) decimation procedure, all high-precision NN potentials flow, as $\Lambda_{\text{low } k} \rightarrow 2.1 \text{ fm}^{-1}$, to a nearly unique low-momentum potential $V_{\text{low } k}$. In this study we consistently employ the N³LO chiral NN potential in deriving $V_{\text{low } k}$.

Given this model of the nuclear interaction in free space, the question remains how to extend the description to a nuclear medium with densities close to that of saturated nuclear matter. It is well known that such two-body interactions alone are unable to reproduce simultaneously the known saturation energy and density of symmetric nuclear matter. The traditional approach is to include a three-nucleon force, but for many of the traditional NN interaction models it is difficult to systematically construct a 3NF that is consistent with the underlying two-body interaction. However, by exploiting the separation of scales in the framework of chiral effective field theory, a systematic and consistent construction of two-, three-, and four-nucleon forces has become possible (for a recent review, see Ref. [21]). The key element there is a power-counting scheme, which orders the contributions in powers of small external momenta over the chiral-symmetry-breaking scale. Long-range effects from multipion exchanges between nucleons are treated explicitly (and calculated within chiral perturbation theory), whereas the short-distance dynamics is encoded in nucleon contact terms. When applied to two- and few-nucleon problems, these chiral potentials are regulated by exponential functions [12,21] with cutoffs ranging from 500 to 700 MeV to eliminate (unphysical) high-momentum components.

The construction of decimated low-momentum three-body forces consistent with the two-body decimation for $V_{\text{low } k}$ is currently a challenge. A common practice is to adjust the parameters of the chiral 3NF so that the binding energies of ³H, ³He, and ⁴He are reproduced. Such a calculation was carried out in Ref. [14] using the Argonne v_{18} [22] low-momentum interaction, where in Table I we restate the values of the low-energy constants c_D and c_E determined in Ref. [14] as a function of $\Lambda_{\text{low } k}$. For a cutoff scale of $\Lambda_{\text{low } k} = 2.3 \text{ fm}^{-1}$, $V_{\text{low } k}$ is only weakly model dependent. Therefore, we expect the values of c_D and c_E derived for the Argonne v_{18} potential at $\Lambda_{\text{low } k} = 2.3 \text{ fm}^{-1}$ to be applicable for the low-momentum N³LO chiral potential employed in the present paper.

B. In-medium nucleon-nucleon interaction

In this section we derive from the leading-order chiral three-nucleon interaction an effective density-dependent in-medium NN interaction. As shown in Ref. [23] the chiral three-nucleon interaction plays an essential role in obtaining the saturation of nuclear matter when using the universal low-momentum NN potential $V_{\text{low } k}$ in Hartree-Fock calculations.

¹This real-valued quantity $T(p', p)$ is often referred to as the K -matrix.

TABLE I. The values of the low-energy constants c_D and c_E of the chiral three-nucleon interaction fit [14] to the binding energies of $A = 3, 4$ nuclei for different values of the momentum cutoff $\Lambda_{\text{low}k}$. The interaction $V_{\text{low}k}$ is derived from the Argonne v_{18} potential.

$\Lambda_{\text{low}k}$ (fm $^{-1}$)	c_D	c_E
2.1	-2.062	-0.625
2.3	-2.785	-0.822

The parameters of its two-pion exchange component, $c_1 = -0.81 \text{ GeV}^{-1}$, $c_3 = -3.2 \text{ GeV}^{-1}$, $c_4 = 5.4 \text{ GeV}^{-1}$, are well determined from fits to low-energy NN phase shifts and mixing angles [12]. If one restricts the two large coefficients $c_{3,4}$ to their (dominant) $\Delta(1232)$ -resonance contributions, the celebrated three-nucleon force of Fujita and Miyazawa [24] is actually recovered. The coupling parameters associated with the one-pion exchange component (c_D) and the short-range contact term (c_E) of the chiral three-nucleon interaction have also been adjusted in Refs. [14,25] to binding energies of three- and four-nucleon systems (${}^3\text{H}$, ${}^3\text{He}$, and ${}^4\text{He}$).

We are considering the (on-shell) scattering of two nucleons in the nuclear medium in the center-of-mass frame, $N_1(\vec{p}) + N_2(-\vec{p}) \rightarrow N_1(\vec{p} + \vec{q}) + N_2(-\vec{p} - \vec{q})$; that is, the total momentum of the two-nucleon system is zero in the nuclear matter rest frame before and after the scattering. The magnitude of the in- and out-going nucleon momenta is $p = |\vec{p}| = |\vec{p} + \vec{q}|$, and $q = |\vec{q}|$ gives the magnitude of the momentum transfer. Having discussed the kinematics, we reproduce first (for the purpose of comparison) the expression for the (bare) one-pion exchange:

$$V_{NN}^{(1\pi)} = -\frac{g_A^2 M_N}{16\pi f_\pi^2} \vec{\tau}_1 \cdot \vec{\tau}_2 \frac{\vec{\sigma}_1 \cdot \vec{q} \vec{\sigma}_2 \cdot \vec{q}}{m_\pi^2 + q^2}. \quad (4)$$

Here, $g_A = 1.27$ denotes the nucleon axial-vector coupling constant, $f_\pi = 92.4 \text{ MeV}$ is the weak pion decay constant, and $m_\pi = 135 \text{ MeV}$ is the (neutral) pion mass. Furthermore, $\vec{\sigma}_{1,2}$ and $\vec{\tau}_{1,2}$ are the usual spin and isospin operators of the two nucleons. Note that we have included an additional factor of $M_N/4\pi$ in V_{NN} to be consistent with the conventions chosen for $V_{\text{low}k}$.

We start with those contributions to the in-medium NN interaction V_{NN}^{med} that are generated by the two-pion exchange component of the chiral three-nucleon force. The three different topologies for (nonvanishing) one-loop diagrams are shown in Fig. 1. The short double line on a nucleon propagator symbolizes the filled Fermi sea of nucleons [i.e., the medium insertion $-2\pi\delta(l_0)\theta(k_f - |\vec{l}|)$ in the in-medium nucleon propagator]. In effect, the medium insertion sums up hole propagation and the absence of particle propagation below the Fermi surface $|\vec{l}| < k_f$. The left diagram in Fig. 1 represents a one-pion exchange with a Pauli-blocked in-medium pion self-energy and the corresponding contribution to V_{NN}^{med} reads

$$V_{NN}^{\text{med},1} = \frac{g_A^2 M_N \rho}{8\pi f_\pi^4} \vec{\tau}_1 \cdot \vec{\tau}_2 \frac{\vec{\sigma}_1 \cdot \vec{q} \vec{\sigma}_2 \cdot \vec{q}}{(m_\pi^2 + q^2)^2} (2c_1 m_\pi^2 + c_3 q^2). \quad (5)$$

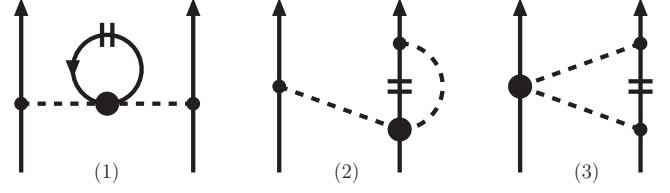


FIG. 1. In-medium NN interaction generated by the two-pion exchange component ($\sim c_{1,3,4}$) of the chiral three-nucleon interaction. The short double line symbolizes the filled Fermi sea of nucleons [i.e., the medium insertion $-2\pi\delta(l_0)\theta(k_f - |\vec{l}|)$ in the in-medium nucleon propagator]. Reflected diagrams are not shown.

The Fermi momentum k_f is related to the nucleon density in the usual way, $\rho = 2k_f^3/3\pi^2$. Since $c_{1,3} < 0$, this term corresponds to an enhancement of the bare one-pion exchange. It can be interpreted in terms of the reduced (spatial) pion decay constant, $f_{\pi,s}^{*2} = f_\pi^{*2} + 2c_3\rho$, in the nuclear medium that replaces f_π^2 in the denominator of Eq. (5). The second diagram in Fig. 1 includes vertex corrections to the one-pion exchange caused by Pauli blocking in the nuclear medium. The corresponding contribution to the in-medium NN interaction has the form

$$V_{NN}^{\text{med},2} = \frac{g_A^2 M_N}{32\pi^3 f_\pi^4} \vec{\tau}_1 \cdot \vec{\tau}_2 \frac{\vec{\sigma}_1 \cdot \vec{q} \vec{\sigma}_2 \cdot \vec{q}}{m_\pi^2 + q^2} \times \left\{ -4c_1 m_\pi^2 [\Gamma_0(p) + \Gamma_1(p)] - (c_3 + c_4) \right. \\ \times [q^2(\Gamma_0(p) + 2\Gamma_1(p) + \Gamma_3(p)) + 4\Gamma_2(p)] \\ \left. + 4c_4 \left[\frac{2k_f^3}{3} - m_\pi^2 \Gamma_0(p) \right] \right\}. \quad (6)$$

Here, we have introduced the functions $\Gamma_j(p)$ that result from Fermi sphere integrals over a (static) pion propagator $[m_\pi^2 + (\vec{l} + \vec{p})^2]^{-1}$:

$$\Gamma_0(p) = k_f - m_\pi \left[\arctan \frac{k_f + p}{m_\pi} + \arctan \frac{k_f - p}{m_\pi} \right] \\ + \frac{m_\pi^2 + k_f^2 - p^2}{4p} \ln \frac{m_\pi^2 + (k_f + p)^2}{m_\pi^2 + (k_f - p)^2}, \quad (7)$$

$$\Gamma_1(p) = \frac{k_f}{4p^2} (m_\pi^2 + k_f^2 + p^2) - \Gamma_0(p) \\ - \frac{1}{16p^3} [m_\pi^2 + (k_f + p)^2] \\ \times [m_\pi^2 + (k_f - p)^2] \ln \frac{m_\pi^2 + (k_f + p)^2}{m_\pi^2 + (k_f - p)^2}, \quad (8)$$

$$\Gamma_2(p) = \frac{k_f^3}{9} + \frac{1}{6} (k_f^2 - m_\pi^2 - p^2) \Gamma_0(p) \\ + \frac{1}{6} (m_\pi^2 + k_f^2 - p^2) \Gamma_1(p), \quad (9)$$

$$\Gamma_3(p) = \frac{k_f^3}{3p^2} - \frac{m_\pi^2 + k_f^2 + p^2}{2p^2} \Gamma_0(p) - \frac{m_\pi^2 + k_f^2 + 3p^2}{2p^2} \Gamma_1(p). \quad (10)$$

By analyzing the momentum- and density-dependent factor in Eq. (6) relative to $V_{NN}^{(1\pi)}$, one finds that this contribution corresponds to a reduction of the one-pion exchange in the nuclear medium. Approximately, this feature can be interpreted in terms of a reduced nucleon axial-vector constant $g_A^*(k_f)$.

The right diagram in Fig. 1 represents Pauli-blocking effects on chiral two-pion exchange. Evaluating it together with the reflected diagram one finds the following contribution to the in-medium NN -interaction:

$$\begin{aligned}
 V_{NN}^{\text{med},3} = & \frac{g_A^2 M_N}{64\pi^3 f_\pi^4} \left\{ -12c_1 m_\pi^2 [2\Gamma_0(p) - (2m_\pi^2 + q^2)G_0(p,q)] \right. \\
 & - c_3 [8k_f^3 - 12(2m_\pi^2 + q^2)\Gamma_0(p) \\
 & - 6q^2\Gamma_1(p) + 3(2m_\pi^2 + q^2)^2 G_0(p,q)] \\
 & + 4c_4 \vec{\tau}_1 \cdot \vec{\tau}_2 (\vec{\sigma}_1 \cdot \vec{\sigma}_2 q^2 - \vec{\sigma}_1 \cdot \vec{q} \vec{\sigma}_2 \cdot \vec{q}) G_2(p,q) \\
 & - (3c_3 + c_4 \vec{\tau}_1 \cdot \vec{\tau}_2) i(\vec{\sigma}_1 + \vec{\sigma}_2) \cdot (\vec{q} \times \vec{p}) \\
 & \times [2\Gamma_0(p) + 2\Gamma_1(p) - (2m_\pi^2 + q^2)(G_0(p,q) \\
 & + 2G_1(p,q))] - 12c_1 m_\pi^2 i(\vec{\sigma}_1 + \vec{\sigma}_2) (\vec{q} \times \vec{p}) \\
 & \times [G_0(p,q) + 2G_1(p,q)] \\
 & + 4c_4 \vec{\tau}_1 \cdot \vec{\tau}_2 \vec{\sigma}_1 \cdot (\vec{q} \times \vec{p}) \vec{\sigma}_2 \cdot (\vec{q} \times \vec{p}) \\
 & \left. \times [G_0(p,q) + 4G_1(p,q) + 4G_3(p,q)] \right\}. \quad (11)
 \end{aligned}$$

One observes that in comparison to the analogous two-pion exchange interaction in vacuum (see Sec. 4.2 in Ref. [26]) the Pauli blocking in the nuclear medium has generated additional spin-orbit terms, $i(\vec{\sigma}_1 + \vec{\sigma}_2) \cdot (\vec{q} \times \vec{p})$, and quadratic spin-orbit terms, $\vec{\sigma}_1 \cdot (\vec{q} \times \vec{p}) \vec{\sigma}_2 \cdot (\vec{q} \times \vec{p})$, written in the last three lines of Eq. (11). The density-dependent spin-orbit terms (scaling with $c_{3,4}$) in the in-medium NN interaction $V_{NN}^{\text{med},3}$ demonstrate clearly and explicitly the mechanism of three-body induced spin-orbit forces proposed long ago by Fujita and Miyazawa [24].

The functions $G_j(p,q)$ appearing in Eq. (11) result from Fermi sphere integrals over the product of two different pion propagators. Performing the angular integrations analytically one arrives at

$$G_{0,*,**}(p,q) = \frac{2}{q} \int_0^{k_f} dl \frac{\{l, l^3, l^5\}}{\sqrt{A(p) + q^2 l^2}} \ln \frac{ql + \sqrt{A(p) + q^2 l^2}}{\sqrt{A(p)}}, \quad (12)$$

with the abbreviation $A(p) = [m_\pi^2 + (l+p)^2][m_\pi^2 + (l-p)^2]$. The other functions with $j = 1, 2, 3$ are obtained by solving a system of linear equations:

$$G_1(p,q) = \frac{\Gamma_0(p) - (m_\pi^2 + p^2)G_0(p,q) - G_*(p,q)}{4p^2 - q^2}, \quad (13)$$

$$\begin{aligned}
 G_{1*}(p,q) = & [3\Gamma_2(p) + p^2\Gamma_3(p) - (m_\pi^2 + p^2)G_*(p,q) \\
 & - G_{**}(p,q)](4p^2 - q^2)^{-1}, \quad (14)
 \end{aligned}$$

$$G_2(p,q) = (m_\pi^2 + p^2)G_1(p,q) + G_*(p,q) + G_{1*}(p,q), \quad (15)$$

$$\begin{aligned}
 G_3(p,q) = & \left[\frac{1}{2}\Gamma_1(p) - 2(m_\pi^2 + p^2)G_1(p,q) \right. \\
 & \left. - 2G_{1*}(p,q) - G_*(p,q) \right] (4p^2 - q^2)^{-1}. \quad (16)
 \end{aligned}$$

In this chain of equations the functions indexed with an asterisk play only an auxiliary role for the construction of $G_{1,2,3}(p,q)$. We note that all functions $G_j(p,q)$ are nonsingular at $q = 2p$ (corresponding to scattering in the backward direction).

Next, we come to the one-pion exchange component of the chiral three-nucleon interaction proportional to the parameter c_D/Λ_χ , where $c_D \simeq -2$ for a scale of $\Lambda_\chi = 0.7$ GeV [14]. The filled black square in the first and second diagrams of Fig. 2 symbolizes the corresponding two-nucleon one-pion contact interaction. By closing a nucleon line at the contact vertex, one obtains a vertex correction (linear in the density ρ) to the one-pion exchange:

$$V_{NN}^{\text{med},4} = -\frac{g_A M_N c_D \rho}{32\pi f_\pi^4 \Lambda_\chi} \vec{\tau}_1 \cdot \vec{\tau}_2 \frac{\vec{\sigma}_1 \cdot \vec{q} \vec{\sigma}_2 \cdot \vec{q}}{m_\pi^2 + q^2}. \quad (17)$$

Since c_D is negative, this term reduces again the bare one-pion exchange, roughly by about 16% at normal nuclear matter density $\rho_0 = 0.16$ fm⁻³. The second diagram in Fig. 2 includes Pauli-blocked (pionic) vertex corrections to the short-range NN interaction. The corresponding contribution to the density-dependent in-medium NN interaction reads

$$\begin{aligned}
 V_{NN}^{\text{med},5} = & \frac{g_A M_N c_D}{64\pi^3 f_\pi^4 \Lambda_\chi} \vec{\tau}_1 \cdot \vec{\tau}_2 \left\{ 2\vec{\sigma}_1 \cdot \vec{\sigma}_2 \Gamma_2(p) \right. \\
 & + \left[\vec{\sigma}_1 \cdot \vec{\sigma}_2 \left(2p^2 - \frac{q^2}{2} \right) + \vec{\sigma}_1 \cdot \vec{q} \vec{\sigma}_2 \cdot \vec{q} \left(1 - \frac{2p^2}{q^2} \right) \right. \\
 & \left. \left. - \frac{2}{q^2} \vec{\sigma}_1 \cdot (\vec{q} \times \vec{p}) \vec{\sigma}_2 \cdot (\vec{q} \times \vec{p}) \right] \right\} \\
 & \times [\Gamma_0(p) + 2\Gamma_1(p) + \Gamma_3(p)], \quad (18)
 \end{aligned}$$

where we have used an identity for $\vec{\sigma}_1 \cdot \vec{p} \vec{\sigma}_2 \cdot \vec{p} + \vec{\sigma}_1 \cdot (\vec{p} + \vec{q}) \vec{\sigma}_2 \cdot (\vec{p} + \vec{q}) = [\dots]$. The ellipses stands for the combination of spin operators written in the square bracket of Eq. (18).

Finally, there is the short-range component of the chiral three-nucleon interaction, represented by a three-nucleon contact vertex proportional to c_E/Λ_χ . By closing one nucleon line (see the right diagram in Fig. 2) one obtains the following

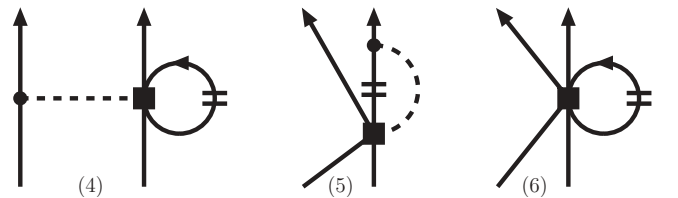


FIG. 2. In-medium NN interaction generated by the one-pion exchange ($\sim c_D$) and short-range component ($\sim c_E$) of the chiral three-nucleon interaction.

contribution to the in-medium NN interaction:

$$V_{NN}^{\text{med},6} = -\frac{3M_{NCE}\rho}{8\pi f_{\pi}^4 \Lambda_{\chi}}, \quad (19)$$

which simply grows linearly in density $\rho = 2k_f^3/3\pi^2$ and is independent of spin, isospin, and nucleon momenta.²

For implementation of the in-medium NN interaction into nuclear structure calculations, the matrix elements of V_{NN}^{med} in the LSJ basis are needed. These are obtained by setting $\vec{\tau}_1 \cdot \vec{\tau}_2 = 4T - 3$, with $T = 0, 1$ the total isospin, and $q = p\sqrt{2(1-z)}$ and performing a projection $\int_{-1}^1 dz P_L(z) \dots$ with Legendre polynomials (for details see Sec. 3 in Ref. [26]). The resulting diagonal spin-singlet ($S = 0, L = J$) and diagonal spin-triplet ($S = 1, L = J - 1, J, J + 1$) matrix elements as well as the off-diagonal mixing matrix elements ($S = 1, L = J - 1, L' = J + 1$) are then functions of the momentum p and k_f (or equivalently the nucleon density ρ). Note that the off-diagonal mixing matrix elements arise exclusively from the tensor operator $\vec{\sigma}_1 \cdot \vec{q} \vec{\sigma}_2 \cdot \vec{q}$ and the quadratic spin-orbit operator $\vec{\sigma}_1 \cdot (\vec{q} \times \vec{p}) \vec{\sigma}_2 \cdot (\vec{q} \times \vec{p})$.

The restriction to on-shell amplitudes greatly simplifies the calculation of the medium-dependent corrections to the nuclear interaction. However, in calculating the shell-model matrix elements one must know the components of the interactions also off shell. That is, one needs to consider $N_1(\vec{p}) + N_2(-\vec{p}) \rightarrow N_1(\vec{p} + \vec{q}) + N_2(-\vec{p} - \vec{q})$, where $p = |\vec{p}|$ and $p' = |\vec{p} + \vec{q}| \neq p$. Rather than calculate the full off-shell in-medium NN interaction, which would give rise to new spin-dependent operators beyond those present in free-space two-nucleon scattering, we look at two prescriptions for extending the on-shell amplitudes off shell. First, we consider the symmetric extrapolation obtained by replacing p^2 in our on-shell expressions with $\frac{1}{2}(p^2 + p'^2)$. Second, we consider the asymmetric extrapolation obtained by simply introducing no explicit dependence on p'^2 . As we discuss later, the largest off-shell dependence comes from $V_{NN}^{\text{med},2}$. In Fig. 3 we compare the two off-shell extrapolations for $V_{NN}^{\text{med},2}$ at $\rho_0 = 0.16 \text{ fm}^{-3}$ in the 1S_0 partial wave to the off-shell dependence of the one-pion-exchange (OPE) low-momentum interaction, where $\Lambda_{\text{low } k} = 2.1 \text{ fm}^{-1}$. We have fixed the value of $p = 0.04 \text{ fm}^{-1}$, and for ease of comparison among the three sets of off-diagonal matrix elements, we have changed the overall sign of the OPE interaction, shifted all three to the origin, and scaled the two medium-dependent interactions so that they coincide with the low-momentum OPE at $p' = 1.6 \text{ fm}^{-1}$. We find that there is excellent agreement between the symmetric off-shell extrapolation and the low-momentum OPE for momenta up to nearly $p' = 1.75 \text{ fm}^{-1}$. Therefore, throughout the remainder of this study we employ only the symmetric off-shell extrapolation.³ This completes our construction of the density-dependent

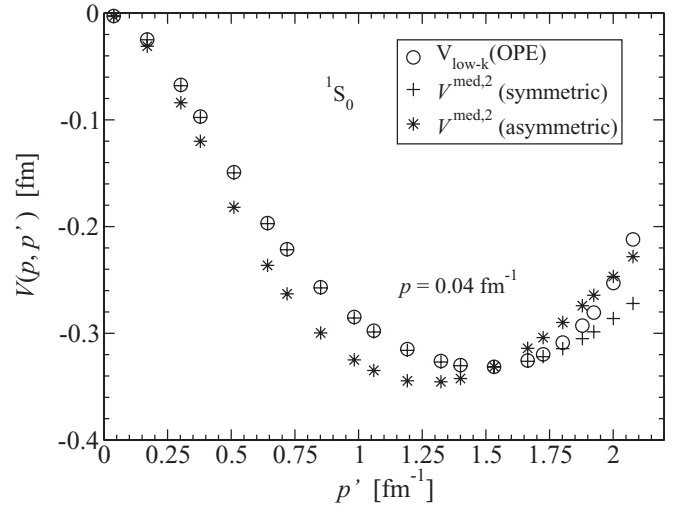


FIG. 3. Two different off-shell extrapolations for the density-dependent $V_{NN}^{\text{med},2}$ at $\rho = \rho_0$ compared to the off-shell dependence of the low-momentum one-pion exchange in the 1S_0 partial wave. Matrix elements are shifted and scaled for comparison purposes (see text for details).

in-medium NN interaction arising from the leading-order chiral three-nucleon force.

III. SHELL-MODEL CALCULATION

A. Formalism

Nowadays there are several computationally intense *ab initio* approaches to solve the nuclear many-body problem for finite nuclei. These include Green function Monte Carlo techniques [27], the no-core shell model [28], and coupled cluster methods [29,30]. However, $A = 14$ nuclei are currently still too complicated for any of these methods to treat exactly. Therefore, in this study we employ the standard shell model, which restricts the allowable configurations to $0\hbar\omega$ but includes the mixing of more complicated configurations through perturbation theory. Indeed, the shell model is expected to provide a good description of light nuclei close to a doubly-magic nucleus (e.g., ^{16}O in the present study).

We describe the states of ^{14}C and ^{14}N as consisting of two $0p$ holes in a closed ^{16}O core. The harmonic oscillator parameter is chosen to be $\hbar\omega = 14 \text{ MeV}$, which yields good agreement with the experimental charge distribution of ^{16}O . The second parameter in the model is the energy splitting between the two $0p$ orbitals, $\epsilon = e(p_{1/2}) - e(p_{3/2}) = 6.3 \text{ MeV}$, which is most accurately obtained from the experimental excitation energy of the first $3/2^-$ state of ^{15}N located 6.3 MeV above the $1/2^-$ ground state.⁴

²To facilitate the computation of symmetry factors and spin and isospin traces, we have modeled (for that purpose) the three-nucleon contact interaction by heavy isoscalar boson exchanges.

³To be consistent with the calculation of $A = 3, 4$ systems in Ref. [14], we have included a regulator function of the form $\exp[-(p/\Lambda_{\text{low } k})^4 - (p'/\Lambda_{\text{low } k})^4]$.

⁴Alternatively, one could calculate microscopically the p -orbit single-particle splitting in perturbation theory. In fact, we have performed second-order calculations of this splitting and find that the density-dependent NN interaction improves the agreement with experiment, though even at nuclear matter saturation density the value

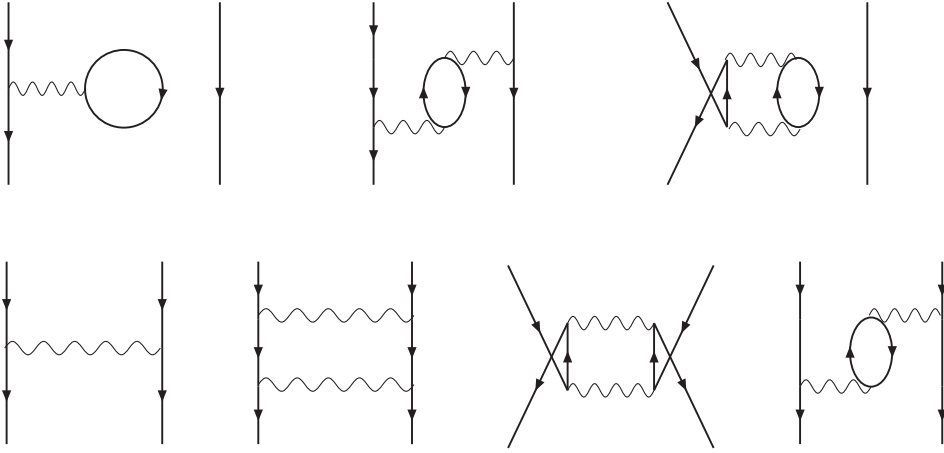


FIG. 4. Diagrams contributing to the effective interaction V_{eff} in our present calculation. Wavy lines represent the density-dependent in-medium nuclear interaction calculated in Sec. II.

To obtain the ground-state energies and wave functions we construct the shell-model effective interaction following the formalism explained in Ref. [18]. The full nuclear many-body problem

$$H\Psi_n = E_n\Psi_n, \quad (20)$$

which presently cannot be solved for mass number $A = 14$, is replaced with a model space problem

$$H_{\text{eff}}\chi_m = E_m\chi_m. \quad (21)$$

In this equation

$$H = H_0 + V \quad \text{and} \quad H_{\text{eff}} = H_0 + V_{\text{eff}}, \quad (22)$$

where H_0 is equal to the sum of the kinetic energy and single-particle harmonic oscillator potential, $E_n = E_n(A = 14) - E_0(A = 16, \text{core})$, and V denotes the input NN interaction (in this case, provided by the density-dependent potential $V_{\text{low}k} + V_{NN}^{\text{med}}$). The effective interaction V_{eff} is obtained from the folded-diagram formalism detailed in Ref. [31]. In the present study, the \hat{Q} -box [31] is calculated by using hole-hole irreducible diagrams of first and second order in $V_{\text{low}k} + V_{NN}^{\text{med}}$ as shown in Fig. 4. To distinguish these many-body particle-hole diagrams from the pion-exchange diagrams contributing to the in-medium NN interaction calculated in Sec. II, we symbolize the input interaction with a wavy line. In previous work [31], the strong short-distance repulsion in the NN S -wave interaction was mitigated by constructing the G -matrix, thereby yielding an effective interaction suitable for perturbation theory techniques. Our present use of low-momentum interactions achieves the same purpose and obviates the construction of the G -matrix. In previous studies [23,32,33] it was found that in general low-momentum interactions are suitable for perturbative calculations. In all of these references satisfactory converged results were obtained by including terms only up to second order in $V_{\text{low}k}$. Moreover, low-momentum interactions are energy independent and do not suffer from possible double counting problems that can arise with G -matrix interactions.

is too small ($\epsilon = 3.6$ MeV). To limit theoretical uncertainties, in all calculations we use the experimental single-particle splitting.

We denote the single-hole states by

$$|1\rangle = |0s_{1/2}^{-1}\rangle, \quad |2\rangle = |0p_{3/2}^{-1}\rangle, \quad |3\rangle = |0p_{1/2}^{-1}\rangle, \quad (23)$$

and the two-hole states coupled to good angular momentum J , isospin T , and parity π are denoted by $|\alpha\beta; J^\pi T\rangle$, where $\alpha, \beta = 2$ or 3 . The matrices to diagonalize are

$$\begin{bmatrix} \vdots \\ \cdots \langle \alpha\beta; 1^+0 | V_{\text{eff}} | \gamma\delta; 1^+0 \rangle \cdots \\ \vdots \end{bmatrix} + \begin{bmatrix} 0 & 0 & 0 \\ 0 & -\epsilon & 0 \\ 0 & 0 & -2\epsilon \end{bmatrix}, \quad (24)$$

for the $J^\pi = 1^+, T = 0$ states, and a similar 2×2 matrix for the $J^\pi = 0^+, T = 1$ states. The ground states for ^{14}C and ^{14}N are, respectively, written as⁵

$$\begin{aligned} \psi_i &= a|22; 0^+1\rangle + b|33; 0^+1\rangle, \\ \psi_f &= x|22; 1^+0\rangle + y|23; 1^+0\rangle + z|33; 1^+0\rangle, \end{aligned} \quad (25)$$

and the reduced Gamow-Teller matrix element M_{GT} is evaluated to be

$$\begin{aligned} M_{\text{GT}} &= \sum_k \langle \psi_f | |\sigma(k)\tau_+(k)| | \psi_i \rangle \\ &= \frac{1}{\sqrt{6}}(-2\sqrt{5}ax + 2\sqrt{2}ay + 4by + 2bz). \end{aligned} \quad (26)$$

The half-life $T_{1/2}$ is inversely proportional to the square of the Gamow-Teller matrix element, and for ^{14}C decay one has

$$T_{1/2} = \frac{1}{f(Z, E_0)} \frac{2\pi^3 \hbar^7 \ln 2}{m_e^5 c^4 G_V^2} \frac{1}{g_A^{*2} |M_{\text{GT}}|^2}, \quad (27)$$

where $E_0 = 156$ keV is the maximum kinetic energy of the emitted electron, $f(Z, E_0)$ is the Fermi integral over phase space, $G_V = G_F \cos \theta_c$ is the weak vector coupling constant, and g_A^* is the in-medium axial vector coupling constant. Although the small end-point energy E_0 of the ^{14}C β decay suppresses the transition by a factor of several hundred, this

⁵We note that the jj -coupling scheme employed in the present paper differs from the previous density-dependent study [8] in which the two-particle states were LS -coupled.

is not nearly sufficient to account for the observed lifetime. To obtain the anomalously long half-life of $T_{1/2} \simeq 5730$ years, the GT matrix element must be anomalously small, $M_{\text{GT}} \simeq 2 \times 10^{-3}$.

B. Results

As a preliminary step, we first calculate the ^{14}C and ^{14}N wave functions, as well as the Gamow-Teller transition matrix element, using the bare $V_{\text{low}k}$ derived from the Idaho N^3LO potential at a cutoff scale $\Lambda_{\text{low}k} = 2.1 \text{ fm}^{-1}$. We find

$$\begin{aligned} |J^\pi = 0^+, T = 1\rangle_1 &= 0.395|22; 0^+, 1\rangle + 0.919|33; 0^+, 1\rangle, \\ |J^\pi = 0^+, T = 1\rangle_2 &= 0.919|22; 0^+, 1\rangle - 0.395|33; 0^+, 1\rangle, \end{aligned} \quad (28)$$

for the two 0^+ states of ^{14}C with energy splitting $\Delta E(0^+) = 12.9 \text{ MeV}$. For the two lowest 1^+ states of ^{14}N we find

$$\begin{aligned} |J^\pi = 1^+, T = 0\rangle_1 &= 0.137|22; 0^+, 1\rangle - 0.676|33; 0^+, 1\rangle \\ &\quad + 0.725|33; 0^+, 1\rangle, \\ |J^\pi = 1^+, T = 0\rangle_2 &= 0.360|22; 0^+, 1\rangle - 0.670|33; 0^+, 1\rangle \\ &\quad - 0.649|33; 0^+, 1\rangle, \end{aligned} \quad (29)$$

where the first excited state lies $\Delta E(1^+) = 2.77 \text{ MeV}$ above the ground state. The second excited $J^\pi = 1^+, T = 0$ state lies nearly 16 MeV higher in energy than the ground state and will therefore be neglected throughout. With these wave functions, the ground state to ground state Gamow-Teller transition matrix element is found to be

$$M_{\text{GT}} = -0.88, \quad (30)$$

which is much too large to describe the known lifetime of ^{14}C .

We now discuss the role of the six density-dependent components V_{NN}^{med} derived in Sec. II that arise from the lowest order chiral 3NF. Indeed, since $A = 14$ nuclei lie just below a double shell closure, we expect the average density experienced by a valence p -shell nucleon to be close to that of saturated nuclear matter. To begin we consider only the matrix elements of these interactions within the $0p^{-2}$ model space. These are shown in Tables II and III for each of the six $V_{NN}^{\text{med},i}$ at the two densities $\rho = \rho_0/10$ and $\rho = \rho_0$. The matrix elements connecting states outside the model space contribute at second order in the diagrammatic expansion of the effective shell-model interaction, V_{eff} , and will be included later. In general, the largest matrix elements are those arising from $V_{NN}^{\text{med},1}$ and $V_{NN}^{\text{med},2}$, which are, respectively, the in-medium pion self-energy and vertex correction resulting from the long-range chiral 3NF. However, we find that to a good approximation they cancel. The same is true for $V_{NN}^{\text{med},4}$ and $V_{NN}^{\text{med},5}$, which are relatively small to begin with. Therefore, we would expect $V_{NN}^{\text{med},3}$ and $V_{NN}^{\text{med},6}$ to be the most important density-dependent corrections to the in-medium NN interaction for the observables considered here.

These observations are made more concrete in the following. As a measure of the strength of the various components contributing to the density-dependent part of the NN interac-

TABLE II. Matrix elements (in units of MeV) between $0p^{-2}$ states coupled to $(J^\pi, T) = (0^+, 1)$ for the six density-dependent contributions to the in-medium NN interaction at the two densities $\rho_0/10$ and ρ_0 .

	$J^\pi = 0^+, T = 1(\rho = \rho_0/10)$		
	$\langle 22 V_{NN}^{\text{med}} 22\rangle$	$\langle 22 V_{NN}^{\text{med}} 33\rangle$	$\langle 33 V_{NN}^{\text{med}} 33\rangle$
1	0.277	0.053	0.240
2	-0.292	-0.071	-0.242
3	0.043	-0.048	0.077
4	-0.054	-0.011	-0.047
5	0.041	0.027	0.022
6	0.171	0.121	0.085
	$J^\pi = 0^+, T = 1(\rho = \rho_0)$		
	$\langle 22 V_{NN}^{\text{med}} 22\rangle$	$\langle 22 V_{NN}^{\text{med}} 33\rangle$	$\langle 33 V_{NN}^{\text{med}} 33\rangle$
1	2.766	0.525	2.395
2	-3.367	-0.714	-2.863
3	1.231	0.004	1.228
4	-0.545	-0.107	-0.469
5	0.458	0.316	0.235
6	1.707	1.207	0.853

tion, we define the quantity

$$R^i(J^\pi, T, \rho) = \sum_{\alpha\beta\gamma\delta} \frac{1}{n} \left| \frac{\langle \alpha\beta J^\pi T | V_{NN}^{\text{med},i} | \gamma\delta J^\pi T \rangle}{\langle \alpha\beta J^\pi T | V_{\text{low}k} | \gamma\delta J^\pi T \rangle} \right|, \quad (31)$$

where ρ is the nuclear density. The sum over α, β, γ , and δ runs over all possible configurations with the allowed spin, isospin, and parity, and n is the number of such configurations (e.g., $n = 3$ for the $J^\pi = 0^+, T = 1$ states). We derive $V_{\text{low}k}$ from the chiral N^3LO NN interaction and choose $\Lambda_{\text{low}k} = 2.1 \text{ fm}^{-1}$. A value of R^i close to 1 indicates that the relevant matrix elements for a particular medium correction are on average equal in magnitude to the matrix elements of $V_{\text{low}k}$ in the given spin-isospin state. We show on the left side of Figs. 5 and 6 the value of R for each of the six density-dependent components of the in-medium nuclear interaction for densities between $\rho = 0$ and $\rho = \rho_0$. The plots on the right-hand side of the two figures include also the ratio R for $V_{NN}^{\text{med},1} + V_{NN}^{\text{med},2}$ and $V_{NN}^{\text{med},4} + V_{NN}^{\text{med},5}$. We see that $V_{NN}^{\text{med},1} + V_{NN}^{\text{med},2}$ as well as $V_{NN}^{\text{med},4} + V_{NN}^{\text{med},5}$ largely cancel, so that the most important contributions from the chiral 3NF are the Pauli-blocked two-pion exchange and the three-nucleon contact interaction proportional to c_E .

Before discussing the results of the full calculation shown at the end of this section, we first obtain a physical understanding of the role played by the two dominant components, $V_{NN}^{\text{med},3}$ and $V_{NN}^{\text{med},6}$, from lowest order perturbation theory. Here the density-dependent components induce small changes in the ground-state wave functions by mixing in the first excited states. This is justified on the basis that the relevant matrix elements of the density-dependent interactions are small compared to the lowest order matrix elements from $V_{\text{low}k}$, as seen in Figs. 5 and 6. We include explicitly the higher

TABLE III. Matrix elements (in units of MeV) between $0p^{-2}$ states coupled to $(J^\pi, T) = (1^+, 0)$ for the six density-dependent contributions to the in-medium NN interaction at the two densities $\rho_0/10$ and ρ_0 .

$J^\pi = 1^+, T = 0(\rho = \rho_0/10)$						
	$\langle 22 V_{NN}^{\text{med}} 22\rangle$	$\langle 23 V_{NN}^{\text{med}} 22\rangle$	$\langle 23 V_{NN}^{\text{med}} 23\rangle$	$\langle 23 V_{NN}^{\text{med}} 33\rangle$	$\langle 22 V_{NN}^{\text{med}} 33\rangle$	$\langle 33 V_{NN}^{\text{med}} 33\rangle$
1	0.299	-0.051	0.128	0.143	-0.121	0.240
2	-0.257	0.091	-0.147	-0.101	0.151	-0.242
3	0.056	0.028	-0.019	-0.015	-0.100	0.182
4	-0.054	0.012	-0.027	-0.023	0.025	-0.047
5	0.034	-0.026	0.012	0.021	-0.040	0.034
6	0.103	-0.107	0.171	-0.002	-0.055	0.089
$J^\pi = 1^+, T = 0(\rho = \rho_0)$						
	$\langle 22 V_{NN}^{\text{med}} 22\rangle$	$\langle 23 V_{NN}^{\text{med}} 22\rangle$	$\langle 23 V_{NN}^{\text{med}} 23\rangle$	$\langle 23 V_{NN}^{\text{med}} 33\rangle$	$\langle 22 V_{NN}^{\text{med}} 33\rangle$	$\langle 33 V_{NN}^{\text{med}} 33\rangle$
1	2.994	-0.505	1.282	1.427	-1.209	2.395
2	-3.193	0.865	-1.718	-1.291	1.589	-2.863
3	0.634	-0.464	0.524	-0.035	-0.927	1.255
4	-0.542	0.123	-0.273	-0.230	0.247	-0.469
5	0.322	-0.286	0.319	0.100	-0.276	0.303
6	1.027	-1.074	1.714	-0.016	-0.550	0.885

order many-body diagrams shown in Fig. 4 at the end of this section.

Given the ground-state wave functions obtained from $V_{\text{low } k}$ alone, as shown in Eqs. (28) and (29), we see that in Eq. (26) the first three terms contributing to the GT matrix element enter with the same sign. It is only the last contribution (bz) that reduces the strength of the transition matrix element. To suppress the GT transition, the density-dependent corrections must therefore shift strength to the $|33\rangle$ components of the wave functions. A straightforward calculation using the matrix elements shown in Tables II and III for $\rho = \rho_0$ gives

$$\begin{aligned} \psi_0^{(1)}(0^+, 1) &= \psi_0^{(0)}(0^+, 1) - 0.0003\psi_1^{(0)}(0^+, 1), \\ \psi_0^{(1)}(1^+, 0) &= \psi_0^{(0)}(1^+, 0) + 0.002\psi_1^{(0)}(1^+, 0) \end{aligned} \quad (32)$$

for the un-normalized perturbed wave functions arising from $V_{NN}^{\text{med},3}$ and

$$\begin{aligned} \psi_0^{(1)}(0^+, 1) &= \psi_0^{(0)}(0^+, 1) - 0.088\psi_1^{(0)}(0^+, 1), \\ \psi_0^{(1)}(1^+, 0) &= \psi_0^{(0)}(1^+, 0) - 0.313\psi_1^{(0)}(1^+, 0) \end{aligned} \quad (33)$$

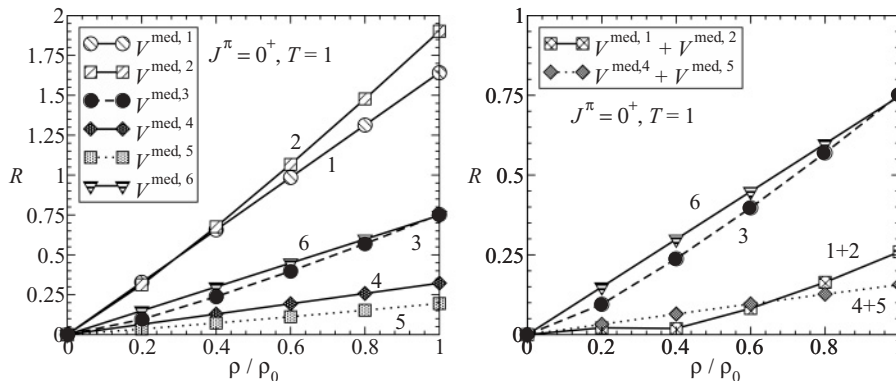


FIG. 5. The average strength of the three $\langle \alpha\beta; 0^+1|V_{NN}^{\text{med},i}|\gamma\delta; 0^+1\rangle$ matrix elements for the six density-dependent contributions to the in-medium NN interaction relative to $V_{\text{low } k}$. The low-momentum interaction is constructed from the Idaho $N^3\text{LO}$ potential for $\Lambda_{\text{low } k} = 2.1 \text{ fm}^{-1}$.

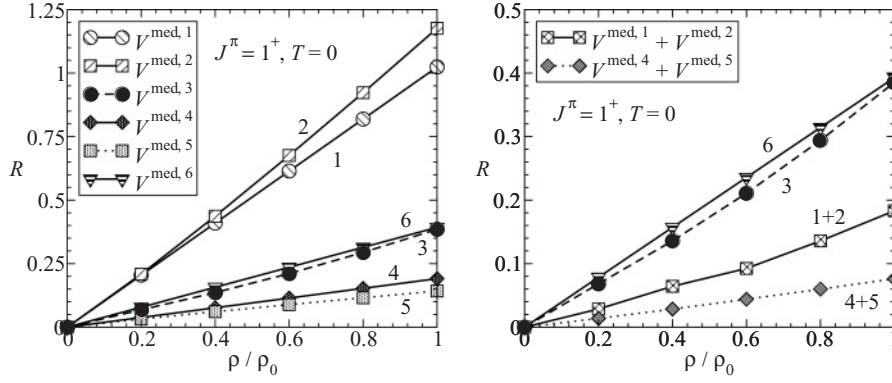


FIG. 6. The average strength of the six $\langle \alpha\beta; 1^+0 | V_{NN}^{\text{med},i} | \gamma\delta; 1^+0 \rangle$ matrix elements for the six density-dependent contributions to the in-medium NN interaction relative to $V_{\text{low}k}$. The low-momentum interaction is constructed from the Idaho $N^3\text{LO}$ potential for $\Lambda_{\text{low}k} = 2.1 \text{ fm}^{-1}$.

The Gamow-Teller transition strength, $B(\text{GT})$, is related to the reduced GT transition matrix element by

$$B(\text{GT}) = (g_A^*)^2 \frac{1}{2J_i + 1} |M_{\text{GT}}|^2 \simeq |M_{\text{GT}}|^2, \quad (34)$$

where $J_i = 0$ and we have used the approximation that the in-medium axial vector coupling constant⁶ $g_A^* \simeq 1$. In general, the effective Gamow-Teller operator has additional terms in a nuclear medium [34,35]:

$$\vec{\mathcal{O}}_{\text{GT,eff}} = g_{LA} \vec{L} + g_A^* \vec{\sigma} + g_{PA} [Y_2, \vec{\sigma}], \quad (35)$$

where \vec{L} is the orbital angular momentum operator and Y_2 denotes the rank-2 spherical harmonic $Y_{2,m}$. However, it is well known from theoretical calculations [36] of the effective GT operator in medium, as well as β -decay calculations [37] performed with phenomenological shell-model effective interactions, that g_{LA} and g_{PA} are almost negligible and that in light nuclei g_A^* is smaller by 15%–20% from its free space value of $g_A = 1.27$ (measured in neutron β decay). In general, one must calculate both the effective interaction V_{eff} and the effective Gamow-Teller operator $\vec{\mathcal{O}}_{\text{GT,eff}}$. In our calculations we assume a 20% reduction of g_A in medium and therefore set $g_A^* = 1.0$.

In Fig. 7 we separate the effects of the six different components of V_{NN}^{med} on the GT strength. When including only the sum of $V_{NN}^{\text{med},1}$, $V_{NN}^{\text{med},2}$, $V_{NN}^{\text{med},4}$, and $V_{NN}^{\text{med},5}$ together with the low-momentum interaction $V_{\text{low}k}$, there is very little density dependence in the calculated GT strength. These four density-dependent components are exactly the terms that are expected to approximately cancel at leading order in the effective shell-model interaction. Including the additional $V_{NN}^{\text{med},3}$, we find that there is a mild increase in the GT strength. This is in accordance with our predictions based on the first-order perturbative calculation of the ^{14}C and ^{14}N ground-state wave functions shown in Eq. (32). However, given the very small mixing of the excited state wave functions at first order, the second-order diagrams contributing to the shell-model effective interaction are equally important. Finally, by including $V_{NN}^{\text{med},6}$ in addition to all other terms, we

find that the GT strength is strongly suppressed. From Eq. (33) our interpretation is that the three-nucleon contact interaction strongly shifts strength to the $|33\rangle$ components of both the ^{14}C and ^{14}N ground-state wave functions, thereby leading to the observed suppression.

In Sec. II we suggested that the symmetric off-shell extrapolation of the density-dependent interaction is preferable to the asymmetric extrapolation, given the former's close agreement with the off-shell behavior of the OPE $V_{\text{low}k}$. In Fig. 8 we study the effect of this choice on the Gamow-Teller strength. Regardless of the off-shell extrapolation method, we find a clear suppression of the $B(\text{GT})$ value for densities close to that of nuclear matter. Indeed, the most important component of the density-dependent NN interaction, $V_{NN}^{\text{med},6}$, is a contact interaction and is therefore independent of the off-shell extrapolation used. We conclude that the error associated with the off-shell prescription is rather small, given that even the extreme asymmetric extrapolation is rather close to the results from the symmetric extrapolation.

Given the strong dependence of the ^{14}C β decay transition rate on the nuclear density, it is important to study how other Gamow-Teller strengths are affected by the inclusion of V_{NN}^{med} .

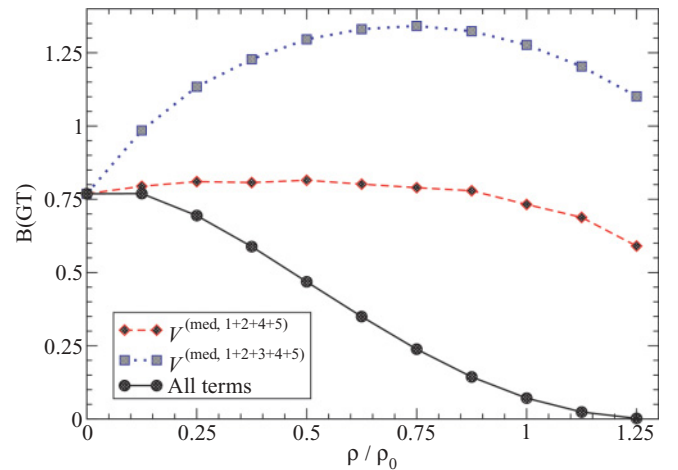


FIG. 7. (Color online) The effects of the various density-dependent contributions to the in-medium NN interaction on the ground state to ground state $B(\text{GT})$ value. The legend denotes which of the $V_{NN}^{\text{med},i}$ are included together with $V_{\text{low}k}$.

⁶At the microscopic level the reduced in-medium g_A^* arises, in the same way as the in-medium NN interaction V_{NN}^{med} , through Pauli-blocked nucleon loops.

TABLE IV. The coefficients of the jj -coupled wave functions defined in Eq. (25) and the associated reduced GT matrix element as a function of the nuclear density ρ .

ρ/ρ_0	a	b	x	y	z	M_{GT}
0.00	0.40	0.92	0.14	-0.68	0.72	-0.877
0.25	0.37	0.93	0.13	-0.67	0.73	-0.833
0.50	0.34	0.94	0.11	-0.63	0.77	-0.684
0.75	0.30	0.95	0.09	-0.57	0.82	-0.488
1.00	0.25	0.97	0.07	-0.49	0.87	-0.267
1.25	0.19	0.98	0.05	-0.41	0.91	-0.045

Recently, GT strengths from the ^{14}N ground state to excited states of ^{14}C have been determined from the experimental charge exchange reaction $^{14}\text{N}(d, ^2\text{He})^{14}\text{C}$ [13]. In Fig. 9 we plot our results for the calculated $B(\text{GT})$ values as a function of the nuclear density ρ . From Fig. 9 one sees that the medium effects improve the agreement between our theoretical calculations and the experimental values for transitions from 0^+ and 1^+ states. The largest effect is clearly a suppression of the ground state to ground state transition for densities at and above that of nuclear matter. The other transition strengths are much less sensitive to the density dependence of the nuclear interaction.

Although we have chosen a low-momentum cutoff scale of $\Lambda_{\text{low}k} = 2.1 \text{ fm}^{-1}$ in these calculations, the value of c_E (and consequently the strength of the important $V_{NN}^{\text{med},6}$ term) depends sensitively on $\Lambda_{\text{low}k}$ as seen in Table I. We therefore calculate the β decay transition strength using also a cutoff scale of $\Lambda_{\text{low}k} = 2.3 \text{ fm}^{-1}$, which incorporates some components of the bare NN interaction unconstrained by elastic NN scattering data but which provides an estimate for the error associated with the chosen momentum cutoff. The results for densities up to $1.25\rho_0$ are shown in Fig. 10 together with the calculations using $\Lambda_{\text{low}k} = 2.1 \text{ fm}^{-1}$. We suggest that this constitutes the most important source of error in our calculation. Moreover, we have studied the dependence

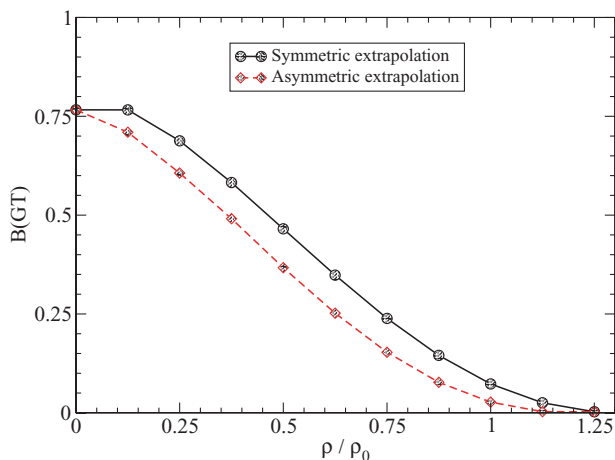


FIG. 8. (Color online) Dependence of the ground state to ground state $B(\text{GT})$ value on the off-shell extrapolation of the density-dependent V_{NN}^{med} interaction. Both the symmetric and asymmetric off-shell extrapolations are shown.

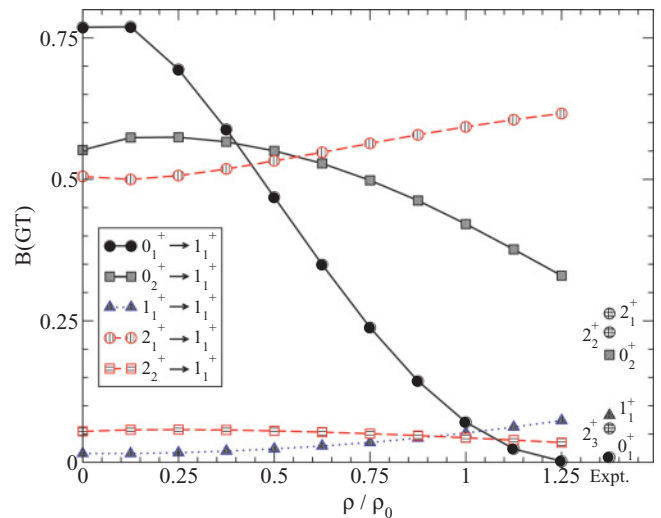


FIG. 9. (Color online) The $B(\text{GT})$ values for transitions from the low-lying states of ^{14}C to the ground state of ^{14}N as a function of the nuclear density. The experimental values are from Ref. [13]. Note that there are three experimental low-lying 2^+ states compared to two theoretical 2^+ states in the $0p^{-2}$ configuration.

of the GT matrix element M_{GT} on the underlying bare NN interaction used in the derivation of $V_{\text{low}k}$. Using the Argonne v_{18} bare potential, we find that changes in M_{GT} are less than 10%. Additional errors include the following: deviations of the effective axial coupling constant g_A^* from 1.0, the choice of the off-shell extrapolation for the in-medium NN scattering amplitudes, and, finally, errors associated with our use of the shell model at second order in perturbation theory. In earlier sections of the paper we have estimated errors associated with the first two approximations, but the last of the three is difficult to quantify. Nevertheless, we expect such errors to be minor, given that previous shell-model calculations (see Ref. [38] and references therein) using $V_{\text{low}k}$ up to second order in

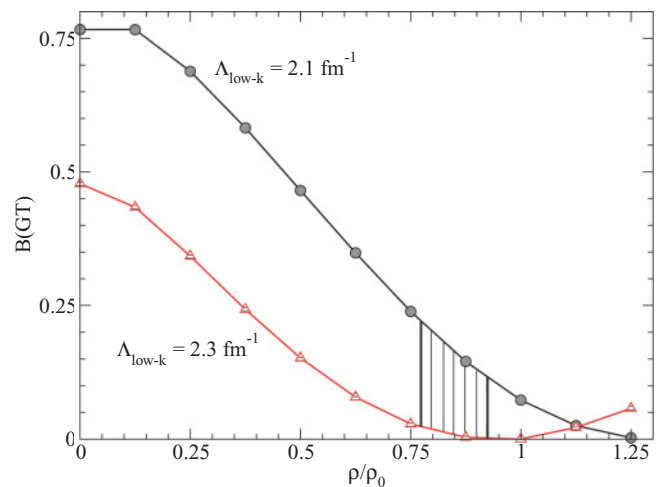


FIG. 10. (Color online) The uncertainty in the calculated value of $B(\text{GT})$ obtained by varying the low-momentum cutoff $\Lambda_{\text{low}k}$ between 2.1 and 2.3 fm^{-1} . The shaded region corresponds to nuclear densities close to that experienced by valence $0p$ -shell nucleons in ^{14}C .

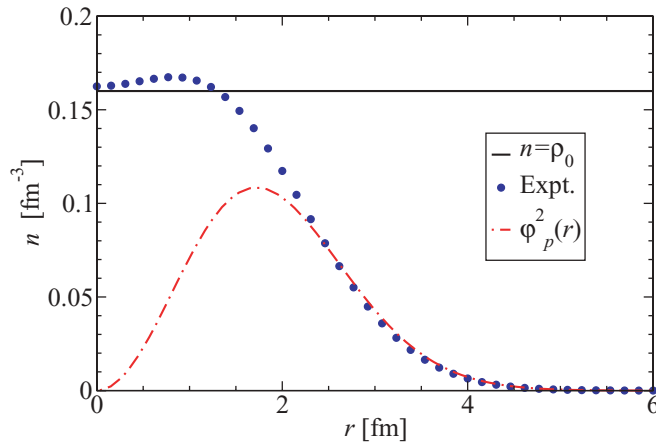


FIG. 11. (Color online) Twice the charge distribution of ^{14}N taken from Refs. [39,40] together with the square of the radial $0p$ -shell wave functions.

perturbation theory have been able to describe very well the properties of nuclei with a small number of valence nucleons above a closed shell.

Because the theoretical value of $B(\text{GT})$ is particularly sensitive to the nuclear density, let us estimate the range over which we expect our calculations to be valid. In Fig. 11 we plot twice the charge distribution of ^{14}N obtained from the fit of the electron scattering experiments [39,40] to the harmonic oscillator density distribution

$$n(r) \propto \left(1 + b \frac{r^2}{d^2}\right) e^{-r^2/d^2}, \quad (36)$$

where for ^{14}N , $b = 1.291$ and $d = 1.740$ fm. We compare this density distribution to the square of the $0p$ -shell radial wave function used in our calculation. This wave function peaks

at a nuclear density of approximately $\rho = 0.85\rho_0$. We have therefore shaded the region of Fig. 10 corresponding to this density $\pm \sim 10\%$.

IV. SUMMARY AND OUTLOOK

We have studied the effects of the leading-order chiral three-nucleon force on the β decay lifetime of ^{14}C , and more generally on the Gamow-Teller transition strengths from the ground state of ^{14}N to the low-lying states of ^{14}C . Our results indicate that the density-dependent in-medium NN interaction V_{NN}^{med} derived from the chiral three-nucleon force has a strong effect on the ground state to ground state transition. In contrast, the GT strengths from the ground state of ^{14}N to the excited states of ^{14}C exhibit only a small density dependence. These results are consistent with the calculations presented in Ref. [8]. We find that the GT strength is particularly sensitive to the genuine short-range component of the chiral 3NF (which is almost completely responsible for driving the suppression) as well as the low-momentum decimation scale $\Lambda_{\text{low}k}$. In general, by fitting the binding energies of $A = 3, 4$ nuclei, one can derive a constraint curve relating the parameters c_D and c_E [41]. Additional information is then required to fix the point on this curve. Recently, it was found in Ref. [42] that the triton GT transition strength is quite sensitive to c_D . Given the sensitivity of the ^{14}C lifetime on the parameter c_E , we suggest that this decay can serve as a useful constraint on the two low-energy constants c_D and c_E once *ab initio* many-body calculations enable study of this problem more accurately.

ACKNOWLEDGMENTS

Work supported in part by BMBF, GSI, and by the DFG cluster of excellence: Origin and Structure of the Universe.

-
- [1] F. Ajzenberg-Selove, J. H. Kelley, and C. D. Nesaraja, Nucl. Phys. **A523**, 1 (1991).
 - [2] W.-T. Chou, E. K. Warburton, and B. A. Brown, Phys. Rev. C **47**, 163 (1993).
 - [3] D. R. Inglis, Rev. Mod. Phys. **25**, 390 (1953).
 - [4] B. Jancovici and I. Talmi, Phys. Rev. **95**, 289 (1954).
 - [5] L. Zamick, Phys. Lett. **21**, 194 (1966).
 - [6] S. Aroua, P. Navrátil, L. Zamick, M. S. Fayache, B. R. Barrett, J. P. Vary, and K. Heyde, Nucl. Phys. **A720**, 71 (2003).
 - [7] B. S. Pudliner, V. R. Pandharipande, J. Carlson, S. C. Pieper, and R. B. Wiringa, Phys. Rev. C **56**, 1720 (1997).
 - [8] J. W. Holt, G. E. Brown, T. T. S. Kuo, J. D. Holt, and R. Machleidt, Phys. Rev. Lett. **100**, 062501 (2008), and references therein.
 - [9] G. E. Brown and M. Rho, Phys. Rev. Lett. **66**, 2720 (1991).
 - [10] G. E. Brown and M. Rho, Phys. Rep. **396**, 1 (2004).
 - [11] D. R. Entem and R. Machleidt, Phys. Rev. C **66**, 014002 (2002).
 - [12] D. R. Entem and R. Machleidt, Phys. Rev. C **68**, 041001(R) (2003).
 - [13] A. Negret *et al.*, Phys. Rev. Lett. **97**, 062502 (2006).
 - [14] A. Nogga, S. K. Bogner, and A. Schwenk, Phys. Rev. C **70**, 061002(R) (2004).
 - [15] S. K. Bogner, T. T. S. Kuo, L. Coraggio, A. Covello, and N. Itaco, Phys. Rev. C **65**, 051301(R) (2002).
 - [16] S. K. Bogner, T. T. S. Kuo, and A. Schwenk, Phys. Rep. **386**, 1 (2003).
 - [17] T. T. S. Kuo, S. Y. Lee, and K. F. Ratcliff, Nucl. Phys. **A176**, 65 (1971).
 - [18] T. T. S. Kuo and E. Osnes, *Folded-Diagram Theory of the Effective Interaction in Nuclei, Atoms and Molecules*, Lecture Notes in Physics, Vol. 364 (Springer-Verlag, New York, 1990).
 - [19] F. Andreozzi, Phys. Rev. C **54**, 684 (1996).
 - [20] E. M. Krenciglowa and T. T. S. Kuo, Nucl. Phys. **A235**, 171 (1974).
 - [21] E. Epelbaum, Prog. Part. Nucl. Phys. **57**, 654 (2006).
 - [22] R. B. Wiringa, V. G. J. Stoks, and R. Schiavilla, Phys. Rev. C **51**, 38 (1995).
 - [23] S. K. Bogner, A. Schwenk, R. J. Furnstahl, and A. Nogga, Nucl. Phys. **A763**, 59 (2005), and references therein.
 - [24] J. Fujita and H. Miyazawa, Prog. Theor. Phys. **17**, 360 (1957).

- [25] E. Epelbaum, *Prog. Part. Nucl. Phys.* **57**, 654 (2006).
- [26] N. Kaiser, R. Brockmann, and W. Weise, *Nucl. Phys.* **A625**, 758 (1997).
- [27] S. C. Pieper and R. B. Wiringa, *Annu. Rev. Nucl. Part. Sci.* **51**, 53 (2001).
- [28] P. Navrátil, J. P. Vary, and B. R. Barrett, *Phys. Rev. C* **62**, 054311 (2000).
- [29] B. Mihaila and J. H. Heisenberg, *Phys. Rev. C* **61**, 054309 (2000).
- [30] D. J. Dean and M. Hjorth-Jensen, *Phys. Rev. C* **69**, 054320 (2004).
- [31] M. Hjorth-Jensen, T. T. S. Kuo, and E. Osnes, *Phys. Rep.* **261**, 125 (1995), and references therein.
- [32] J. D. Holt, J. W. Holt, T. T. S. Kuo, G. E. Brown, and S. K. Bogner, *Phys. Rev. C* **72**, 041304(R) (2005).
- [33] L. Coraggio, A. Covello, A. Gargano, N. Itaco, and T. T. S. Kuo, *Phys. Rev. C* **75**, 057303 (2007).
- [34] A. Arima and L. J. Huang-Lin, *Phys. Lett.* **B41**, 429 (1972); **B41**, 435 (1972).
- [35] B. Castel and I. S. Towner, *Modern Theories of Nuclear Moments* (Clarendon Press, Oxford, 1990).
- [36] I. S. Towner, *Phys. Rep.* **155**, 263 (1987).
- [37] B. A. Brown and B. H. Wildenthal, *Nucl. Phys.* **A474**, 290 (1987).
- [38] L. Coraggio, A. Covello, A. Gargano, N. Itaco, and T. T. S. Kuo, *Prog. Part. Nucl. Phys.* **62**, 135 (2009).
- [39] L. A. Schaller, L. Schellenberg, A. Ruetschi, and H. Schneuwly, *Nucl. Phys.* **A343**, 333 (1980).
- [40] W. Schütz, *Z. Phys. A* **273**, 69 (1975).
- [41] P. Navrátil, V. G. Gueorguiev, J. P. Vary, W. E. Ormand, and A. Nogga, *Phys. Rev. Lett.* **99**, 042501 (2007).
- [42] D. Gazit, S. Quaglioni, and P. Navrátil, arXiv:0812.4444.